Scripta Materialia 171 (2019) 6–9

Contents lists available at ScienceDirect

Scripta Materialia

journal homepage: www.elsevier.com/locate/scriptamat

Stishovite formation at very low pressures in soda-lime glass

Marta Pozuelo [a], Joseph Lefebvre [b], Pratyush Srivastava [c], Vijay Gupta [c,*]

[a] Department of Materials Science and Engineering, University of California Los Angeles, Los Angeles, CA 90095, USA
[b] Hysitron, Inc., Minneapolis, MN 55344, USA
[c] Department of Mechanical and Aerospace Engineering, University of California Los Angeles, Los Angeles, CA 90095, USA

ARTICLE INFO

Article history:
Received 29 April 2019
Accepted 2 June 2019
Available online xxxx

Keywords:
Soda lime glass
Nanopillars
Nano compression
Polymorphic transformation
High resolution transmission electron microscopy (HRTEM)

ABSTRACT

We show for the first time that amorphous soda-lime glass undergoes polymorphic transformation to its densest crystalline stishovite phase at only ~5 GPa of pressure and room temperature, by uniaxially compressing the soda-lime glass nanopillars of 500 nm diameter and observing the post-deformed pillars under transmission electron microscopy. This contrasts with the recent shock-compression experiments of amorphous fused silica glass plates which report a pressure threshold of 34 GPa for stishovite formation. Our findings support recent dislocation dynamics simulations on W pillars which show that small domain size acts as a proxy for high temperature, thereby reducing the pressure threshold.

Highly dense and ultra-hard stishovite phase is the most stable form of silicon dioxide (SiO_2). It is formed under extreme conditions of temperature and pressure. Small quantities of stishovite were first found in nature in intensely shocked quartz sandstone at Meteor Crater in Arizona [1]. Microcrystals of Stishovite were also discovered as inclusions in amorphous silica grains in shocked melt pockets of a lunar meteorite [2]. Stishov and Popova [3] were the first to synthesize this phase in 1961 by statically compressing silica above 160,000 atm at 1200–1400 °C. Recently, stishovite has been formed by shock-loading of SiO_2 phases under very high pressures (>34 GPa) by simulating the conditions under which it is formed in nature [4,5]. Molecular Dynamics simulations have provided more mechanistic details of this transformation and have confirmed that stishovite becomes the most stable polymorph of SiO_2 under very high pressure ~50 GPa under shock conditions [6]. In this communication, we report nucleation of the stishovite phase in soda-lime glass (SLG) at room temperature at a remarkably low compressive stress of only 4.8 GPa. We attribute this unusual observation to the presence of high shear stresses which induce diffusion of Na^+ and Ca^{2+} cations within the intensely sheared regions of SLG to create localized cation-free regions to allow nucleation of the stishovite phase. Practical implications of this observation are somewhat counter-intuitive in that SLG with a density of 2.6 g/cm^3 can be used as an armor material for protection against ballistic impacts as the transformation to the much denser stishovite phase (4.3 g/cm^3) should consume an enormous amount of impact energy by undergoing almost 40% volume compression [7,8].

The surprising observations in SLG were uncovered while studying the effect of size in polymorphic transformations in pure SiO_2 glasses through uniaxial compression of sub-micrometer diameter SiO_2 pillars using a microindenter stationed inside a scanning electron microscope (SEM). The small pillar diameter allowed generation of very high pressures which in previous studies were generated through triaxial compression of macroscopic samples inside a diamond anvil cell. In contrast to the diamond anvil cell where the glass is subjected to a state of pure pressure, the pillar material in our experiments is subjected to both pressure and shear as the pillars can expand laterally when compressed along their longitudinal axis by the indenter head. Focused Ion Beam (FIB) was used to machine sub-micron pillars of approximately 400 nm in diameter on a commercially available thin SLG microscope slide. SEM images of the as-fabricated pillars in Figs. 1A and 2A show the characteristic tapering and rounded tip that are known to result from FIB milling. These amorphous SLG pillars were compressed *in-situ* along their axis using a nanoindenter which was installed inside the SEM. More details about *in-situ* nanocompression tests can be found in the Supplementary Videos 1 and 2. Fig. 3 shows representative engineering stress-strain plots for the two SLG pillars at room temperature when loaded at a strain rate of 10^{-3} s^{-1}. After reaching a peak stress of around 1000 MPa, both pillars show a remarkable capacity for plastic deformation, accommodating almost ~60% strain, with no evidence of any fracture. Figs. 1B and 2B show SEM images of the deformed pillars. A maximum stress of 4.8 GPa and 4.2 GPa was calculated for pillars 1 and 2, respectively, by using their mid-height diameters. Besides the unusual plastic deformation, both pillars show a remarkable strain hardening effect which cannot be attributed to pillar tapering alone. This might be indicative of the formation of a much harder phase during

* Corresponding author.
E-mail address: vgupta@ucla.edu (V. Gupta).

https://doi.org/10.1016/j.scriptamat.2019.06.005
1359-6462/

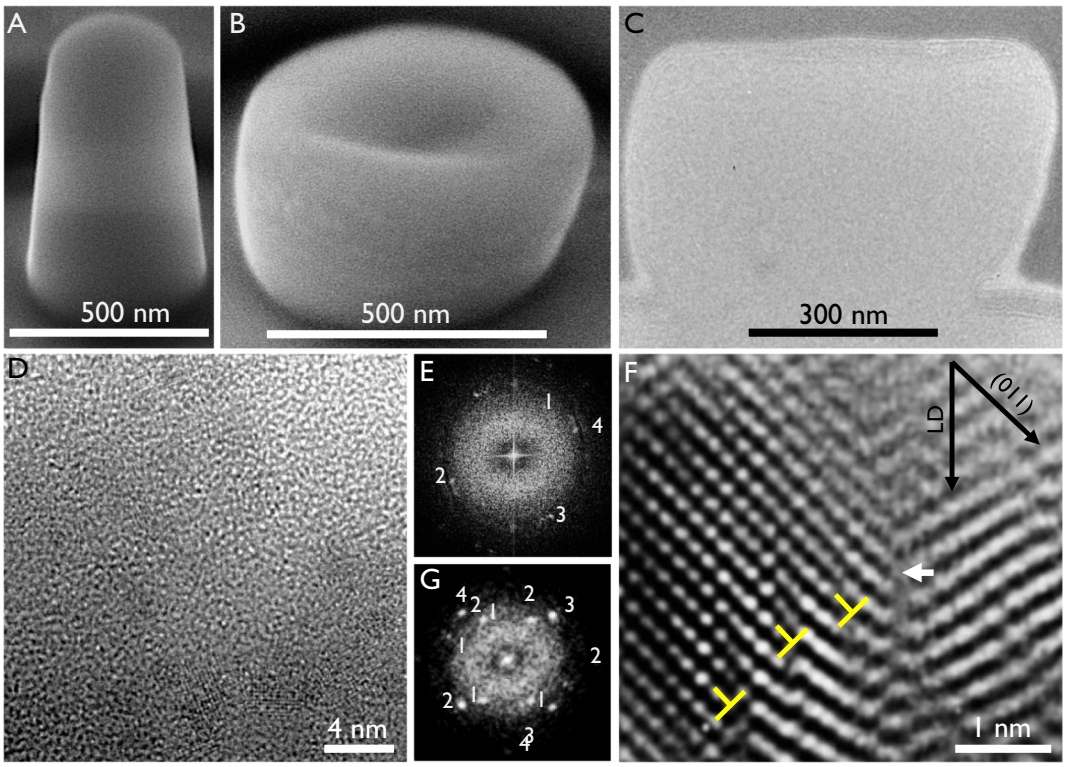

Fig. 1. Stishovite formation in a sub-micron glass pillar after 4.8 GPa of compressive stress. A, B, 35° tilted-view SEM images of glass pillar 1 before and after compression test. C, Thinfilm FIB prepared from the compressed pillar shown in B. D, High-resolution TEM image from the center of the pillar showing nanocrystalline regions in the compressed amorphous matrix. E, Fast Fourier transform (FFT) of the image shown in D displaying some crystalline spots in addition to the amorphous rings. F, Fourierfiltered atomicresolution TEM image of Stishovite phase as reveals its FFT shown in G. Interplanar spacing measurements from E and G are collected in Table 1. Note edge dislocations (marked in yellow) located on the {011} planes of the Stishovite. (For interpretation of the references to colour in this figure legend, the reader is referred to the web version of this article.)

compression. This was further investigated by analyzing the microstructure of the deformed pillars by high-resolution transmission electron microscopy (HRTEM).

TEM samples from top to bottom of the compressed pillars were prepared by FIB as shown in Figs. 1C and 2C. These images reveal that excessive compression is accommodated inside the pillars through the formation of localized shear bands which are visible at the pillar surface as indicated by black arrows in Figs. 1C and 2C.

Using HRTEM and Fast Fourier Transform (FFT) analysis, we confirmed the presence of nanocrystalline regions, about 4 nm in size, distributed within an amorphous matrix (Fig. 1D). Its indexed FFT in Fig. 1E reveals four diffraction spots in addition to the amorphous rings. We have identified these crystalline phases as stishovite by comparing the experimentally measured interplanar spacings (Table 1) with those expected for the tetragonal stishovite [9]. The relative errors between the measured and tabulated interplanar spacings (Table 1) are quite low which further confirm our main finding. Two stishovite crystals separated by a grain boundary (highlighted by a white arrow) can be observed in the atomic resolution TEM image in Fig. 1F as confirmed by its indexed FFT (Fig. 1G). Their corresponding interplanar spacing measurements are also collected in Table 1. It is interesting to note that edge dislocations (marked in yellow) are located on the {011} planes of the stishovite suggesting a deformed stishovite crystal during compression, where the slip planes are oriented about 45° with respect to the loading direction (LD). In addition to finding the stishovite crystals within the pillar volume, we also found them just below the base of

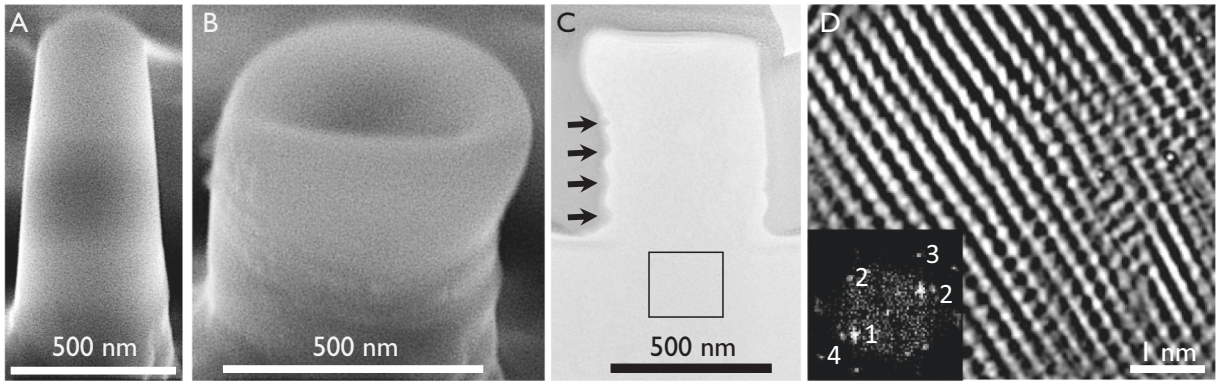

Fig. 2. Stishovite formation in a sub-micron glass pillar after 4.2 GPa of compressive stress and in the glass substrate underneath. A and B, 35° tilted-view SEM images of glass pillar 2 before and after compression test. C, TEM sample prepared by FIB from the compressed pillar shown in B. Shear bands are visible at the pillar surface indicated by black arrows. D, High-resolution TEM image of the substrate region highlighted by a square in C. Inset is its FFT showing diffraction spots corresponding to Stishovite phase as confirmed by their interplanar spacing measurements collected in Table 1.

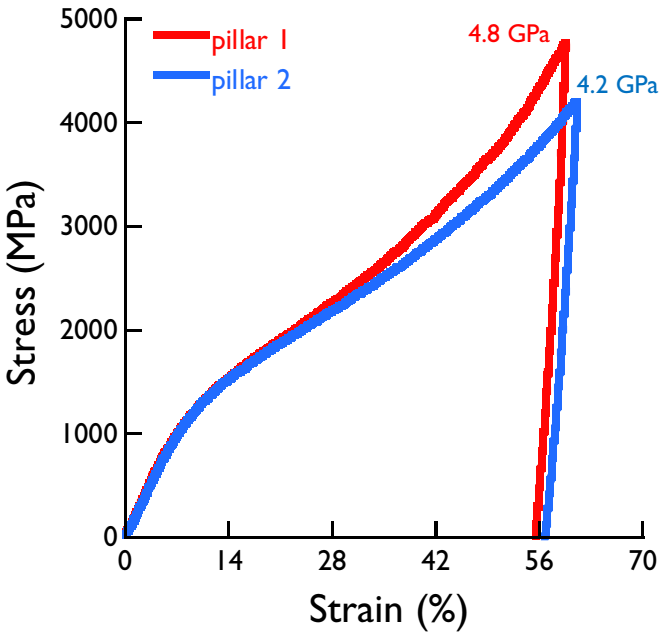

Fig. 3. *In-situ* SEM nanocompression tests of sub-micron glass pillars. Engineering compressive stress-strain curves reaching 4.8 and 4.2 GPa as the maximum compressive stress at around 60% of strain for pillars 1 and 2, respectively.

the compressed pillars inside the SLG substrate. Fig. 2D shows the HRTEM image of one such region below Pillar 2. Its indexed FFT (as inset) and their interplanar spacing measurements (Table 1) confirm that this crystalline phase also corresponds to stishovite.

We are aware of the effects of the electron beam irradiation that can promote crystallization in some amorphous materials such as Si film doped with impurities [10]. To rule out this effect, we studied the effect of electron beam irradiation on the initial amorphous SLG sample by subjecting it to different electron beam exposure times (0, 7 and 12 min). TEM examination did not reveal the presence of any crystalline phases (see Supplementary Figure). Therefore, any possible effect of the electron beam irradiation on crystallization can be conclusively ruled out in our work.

We are unable to directly compare our observations of very low stishovite nucleation stress to any prior experimental or simulation studies on SLG. However, this phenomenon has been thoroughly investigated in fused silica over the last several decades. The most recent conclusive study on this topic by Tracy et al. [11] showed that shock compression of fused silica below 34 GPa results in a 4 to 6-coordinated dense amorphous structure rather than a mixed-phase (crystalline) region as previously theorized and that it is only beyond 34 GPa that there is the requisite thermal energy to transform fused silica into polycrystalline stishovite. Unlike previous efforts which examined post-shocked samples, Tracy et al.[11] used *in situ* X-ray diffraction to analyze the changes in the fused silica structure during shock compression of the sample by a high velocity plate impact setup. The transformation from highly coordinated amorphous phase into the crystalline stishovite structure on shock compression time scales of few nanoseconds suggests that such transformations arise from local correlated motions of atoms as opposed to longer length scale diffusive rearrangements. This is consistent with the MD simulation work of Shen et al. [12] which supports formation of stishovite within nanosecond time-scale.

Table 1
Interplanar spacing measured from FFTs and comparison with the tabulated values for Stishovite.

#	*d* measured (nm)	*d* Stishovite (nm)	hkl	Int (%)	Error (%)
		FFT data from Fig. 1E			
1	0.29	0.2958	110	100	2.0
2	0.25	0.2600	001	7	3.8
3	0.22	0.2249	011	22	2.2
4	0.20	0.1981	111	38	1.0
		FFT data from Fig. 1G			
1	0.30	0.2958	110	100	1.4
2	0.22	0.2249	011	22	2.2
3	0.20	0.1981	111	38	1.0
4	0.15	0.1531	121	37	2.0
		FFT data from Fig. 2D			
1	0.29	0.2958	110	100	2.0
2	0.22	0.2249	011	22	2.2
3	0.20	0.1981	111	38	1.0
4	0.15	0.1531	121	37	2.0

The extremely low stishovite nucleation stress in SLG compared to that in fused silica of 34 GPa is very surprising especially because in SLG in addition to atomic rearrangement one must also move the Na^{+} and Ca^{2+} ions to create cation-free regions into which pure stishovite crystals can be nucleated. Thus, we require both high local stresses for enhanced atomic mobility as well as diffusion of Ca and Na ions to create cation-free regions. Interestingly, there is support for both these mechanisms as discussed below.

For amorphous materials such as metallic glasses, the plastic deformation at room temperature is characterized by the formation and movement of highly localized shear bands [13,14]. It has been suggested that the plastic flow within the shear bands destroys the short-range compositional order existent in the glass [15]. It can be understood as mechanical deformation-induced crystallization as reported for Al-based metallic glasses [16]. In this case, the large plastic strain during mechanical milling induces atomic displacements and enhanced atomic mobility. Therefore, plastic flow in silicate glasses requires shear deformation involving the breaking of interatomic bonds and the formation of new bonds (equivalent to dislocation motion in metals) or densification, which involves simply a collapse of the structure into a more close-packed arrangement by minor bond rotation and changes of bond angles [17]. Such a mechanism is clearly plausible in the intensely sheared regions of SLG in our experiments.

It is well known that among the three types of crystallization of amorphous solids, (primary crystallization, eutectic and polymorphous), primary crystallization requires atomic diffusion due to the large compositional difference between the amorphous phase and its crystallized product [18,19]. SLG contains about 16 wt% Na in the form of Na_2O and 10 wt% Ca in the form of CaO in addition to SiO_2 [13,20,21]. Therefore, during crystallization of stishovite from SLG, atomic diffusion of cations such as Na^{+} and Ca^{2+} might be involved due to the large compositional difference between the amorphous SLG (SiO_2-NaO_2-CaO-….) and crystalline stishovite (SiO_2).

Previous studies on cation diffusion in SLG have reported that Na^{+} ions are always more mobile than the Ca^{2+} ions [22,23]. The peculiar diffusion behavior of Ca^{2+} is explained based on the formation of dissimilar Na—Ca pairs in soda lime silicates observed by nuclear magnetic resonance (NMR) studies [23]. We believe that the formation of these Na—Ca bonds provides the SLG with localized cation-free regions, where the stishovite phase can be formed. That would explain why the stishovite transformation is not uniform along the entire pillar but only in localized regions within the pillar as well as in the substrate just below the pillar.

In summary, we have demonstrated for the first time that small domain size can substantially reduce the pressure threshold for transformation at room temperature to the highly dense stishovite phase in SLG.

Commercial SLG in the form of thin microscope cover slip was used for this study. Sub-micron glass pillars around 400 nm in diameter and aspect ratio between 1:2 and 1:3 were machined from the SLG by Focused Ion Beam (FIB). The FEI Nano 600 dual beam Scanning Electron Microscope/Focused Ion Beam (SEM/FIB) was used for this purpose. A series of concentric annular milling patterns with different currents were applied to minimize the tapering.

Microcompression tests were conducted at room temperature under displacement control mode and at a strain rate of 10^{-3} s^{-1} using a PI 85 SEM PicoIndenter (Hysitron Inc.) with a 5μm flat punch diamond probe. In order to avoid any overestimation of the measured stress due to pillar tapering, diameter at half-height was used to estimate the stress inside the pillars.

Thin foil TEM samples from the compressed pillars were prepared by FIB. TEM analysis was carried out using a FEI-Titan Scanning/Transmission Electron Microscope (STEM) operating at 300 kV.

Supplementary data to this article can be found online at https://doi.org/10.1016/j.scriptamat.2019.06.005.

Acknowledgments

This work was funded by the Office of Naval Research (ONR) under contract No. N00014-17-1-2490 for which we are grateful to Dr. Roshdy Barsoum of that agency. The authors are particularly grateful to Prof. S. Tolbert for her discussions on silicate glasses and to N. Bodzin for his assistance with TEM samples preparation by FIB.

Author contributions

M.P. performed the TEM characterization. M.P. and P.S. analyzed the data. J.L. conducted the *in situ* nanocompression tests. M.P., P.S., and V.G. wrote the manuscript. V.G. conceived the idea and supervised the work.

References

[1] E.C.T. Chao, J.J. Fahey, J. Littler, D.J.J. Milton, Geophysical Res. 67 (1962) 419–421.
[2] E. Ohtani, S. Ozawa, M. Miyahara, Y. Ito, T. Mikouchi, M. Kimura, T. Arai, K. Sato, K. Hiraga, PNAS 108 (2011) 463–466.
[3] S.M. Stishov, S.V. Popova, Geokhimiya 10 (1961) 837–839.
[4] A. Salleo, S.T. Taylor, M.C. Martin, W.R. Panero, R. Jeanloz, T. Sands, F.Y. Génin, Nature Mater. 2 (2003) 796–800.
[5] O. Tschauner, S.-N. Luo, P.D. Asimow, T.J. Ahrens, Am. Mineral. 91 (2006) 1857–1862.
[6] M. Grujicic, J. Snipes, S. Ramaswami, R. Yavari, B.J. Cheeseman, *Nanomaterials* 650625, 2015.
[7] Barsoum, 29th International Symposium on Ballistics, 2016.
[8] M. Grujicic, et al., J. Mater. Eng. Performance 24 (2015) 4890–4907.
[9] R. Chakraborty, A. Dey, A.K. Mukhophadhyay, Met. Mater. Trans. 41 (2010) 1301–1312.
[10] E. Kilinc, R.J.J. Hand, Non-Cryst. Solids 429 (2015) 190–197.
[11] S.J. Tracy, S.J. Turneaure, T.S. Duffy, 135702–1-6, 2018.
[12] Y. Shen, S.B. Jester, T. Qi, E.J. Reed, Nat. Mater. 15 (2016) 60–65.
[13] D.R. Allen, J.C. Foley, J.H. Perepezko, Acta Mater. 46 (1998) 431–440.
[14] Y. He, G.J. Shiflet, S.J. Poon, Acta Metall. Mater. 43 (1995) 83–91.
[15] F. Ye, K. Lu, Phys. Review B 60 (1999) 7018–7024.
[16] W.-Q. Huang, S.-R. Liu, Z.-M. Huang, T.-G. Dong, G. Wang, C.-J. Qin, Sci. Reports 4 (2015) 1–6.
[17] F. Spaepen, Acta Metall. 25 (1977) 407–415.
[18] M. Gogebakan, P.J. Warren, B. Cantor, Mater. Sci. Eng. A 226-228 (1997) 168–172.
[19] C.A. Pampillo, H.S. Chen, Mater. Sci. Eng. 13 (1974) 181–188.
[20] F.M.J. Ernsberger, Ame. Cer. Soc. 51 (1968) 545–547.
[21] A. Kubota, M.-J. Caturla, L. Davila, et al., Proc. SPIE 4679 (2002) 108–116.
[22] F.V. Natrup, H. Bracht, S. Murugavel, B. Roling, Phys. Chem. Chem. Phys. 7 (2005) 2279–2286.
[23] S.K. Lee, J.F.J. Stebbins, Phys. Chem. B 107 (2003) 3141–3148.